Photochromism of rare-earth metal-oxy-hydrides

Nafezarefi, F.; Schreuders, H.; Dam, B.; Cornelius, S.

DOI
10.1063/1.4995081

Publication date
2017

Document Version
Final published version

Published in
Applied Physics Letters

Citation (APA)
Nafezarefi, F., Schreuders, H., Dam, B., & Cornelius, S. (2017). Photochromism of rare-earth metal-oxy-hydrides. *Applied Physics Letters*, *111*(10), 1-5. Article 103903. https://doi.org/10.1063/1.4995081

Photochromism of rare-earth metal-oxy-hydrides

F. Nafezarefi, H. Schreuders, B. Dam, and S. Cornelius[a)]
Materials for Energy Conversion and Storage, Department of Chemical Engineering, Delft University of Technology, Van der Maasweg 9, NL-2629HZ Delft, The Netherlands

(Received 10 July 2017; accepted 24 August 2017; published online 8 September 2017)

Recently, thin films of yttrium oxy-hydride (YO_xH_y) were reported to show an unusual color-neutral photochromic effect promising for application in smart windows. Our present work demonstrates that also oxy-hydrides based on Gd, Dy, and Er have photochromic properties and crystal structures similar to YO_xH_y. Compared to YO_xH_y, the optical bandgaps of the lanthanide based oxy-hydrides are smaller while photochromic contrast and kinetics show large variation among different cations. Based on these findings, we propose that cation alloying is a viable pathway to tailor the photochromic properties of oxy-hydride materials. Furthermore, we predict that the oxy-hydrides of the other lanthanides are also potentially photochromic. *Published by AIP Publishing.* [http://dx.doi.org/10.1063/1.4995081]

Upon hydrogenation, yttrium shows a metal insulator transition accompanied by dramatic changes in optical and electrical properties.[1] Pd capping of Y thin films allows for a reversible (de)hydrogenation.[2,3] The optical changes involved in the (de)hydrogenation process lead to intriguing findings such as the switchable mirror effect in YH_x.[4] Depending on the H concentration, the Y-H system exhibits three structural phases. Upon hydrogenation, metallic Y with a hexagonal structure transforms into the cubic dihydride phase (β-$YH_{1.9–2.1}$) and finally the hexagonal trihydride phase (γ-$YH_{2.7–3}$).[1] While the $YH_{1.9+\delta}$ phase is a black and opaque metal, the trihydride is a transparent semiconductor with a direct optical bandgap of 2.6 eV.[5] A unique photochromic effect was recently observed in magnetron sputtered YO_xH_y thin films after excitation by an AM1.5 solar spectrum at room temperature and ambient pressure.[6] This polycrystalline semiconductor has an optical bandgap of about 2.6 eV and an fcc crystal structure with a lattice constant of 5.35–5.40 Å.[7,8] The initially transparent material photodarkens in a wide spectral range covering the visible (VIS) and near infrared (NIR) with a time constant in the order of minutes.[6] Hence, YO_xH_y is a promising material for application in energy saving smart windows and other chromogenic devices. Most photochromic materials are organic in nature and exhibit narrow spectral absorption bands together with fast switching behavior.[9–11] However, due to limited stability vs. oxygen, humidity, and heat, as well as ultra-violet (UV) irradiation induced fatigue,[11] complex processing is often required to tailor the photochromic response and to enhance the product lifetime. In contrast, inorganic photochromic materials have the potential for higher physico-chemical stability and show much broader absorption bands, resulting in color-neutral photochromism, albeit at lower switching speed. A well-known example of inorganic photochromic materials are silver halide doped glasses where the photochromic effect is based on the reversible formation of plasmonic nanoparticles.[12,13] While the photochromic mechanism in YO_xH_y remains to be uncovered, Mongstad *et al*. suggested that the fcc crystal structure and the presence of oxygen are essential for the photochromic effect.[6,14]

In this work, we investigate the structural and optical properties of rare-earth metal based oxy-hydrides in comparison to YO_xH_y. The lanthanides show physical and chemical behavior very similar to Y in terms of mostly trivalent oxidation state, ionic radius, as well as crystal structure and properties of compounds formed with oxygen and hydrogen. Indeed, we find that the oxy-hydrides of Gd, Dy, and Er are photochromic. This allows us to explore possible structural and chemical effects on the photochromic properties of the MO_xH_y material family. Interestingly, we observe (i) lower optical bandgaps of the rare-earth oxy-hydrides compared to YO_xH_y, (ii) a large variation of photochromic kinetics for different M, and (iii) exceptionally strong photochromism in GdO_xH_y particularly in the NIR spectral region. Moreover, it is demonstrated that the formation of transparent photochromic MO_xH_y thin films only takes places above a certain critical value of the total pressure during reactive sputter deposition.

A series of yttrium and rare-earth (Gd, Dy, Er) based thin films was prepared on unheated UV-grade fused silica (f-SiO_2) substrates by reactive direct current magnetron sputtering of 2-inch metal targets (99.9% purity) at 100 W in an Ar/H_2 gas mixture (5N purity) with 12.5 vol. % of H_2. The deposition system was kept at a base pressure below 3×10^{-6} Pa and the total pressure, p, during deposition was varied by means of a butterfly reducing valve mounted at the turbo molecular pump inlet. Structural, optical, and photochromic properties were investigated by a combination of X-ray diffraction (XRD), optical spectroscopy, and UV excitation.

In contrast to what was previously reported by Mongstad *et al*.,[6,7] we do not always obtain transparent and photochromic films after reactive sputtering of Y in Ar/H_2 mixtures followed by exposure to air. Uncapped films prepared below a certain critical deposition pressure remain dark metallic upon exposure to air. These films are not photochromic and show a low transmittance over the entire spectral range, except for a narrow region in red part of the visible spectrum (Fig. 1).

[a)]Author to whom correspondence should be addressed: s.cornelius@tudelft.nl. Tel: +31(0)1527-87391.

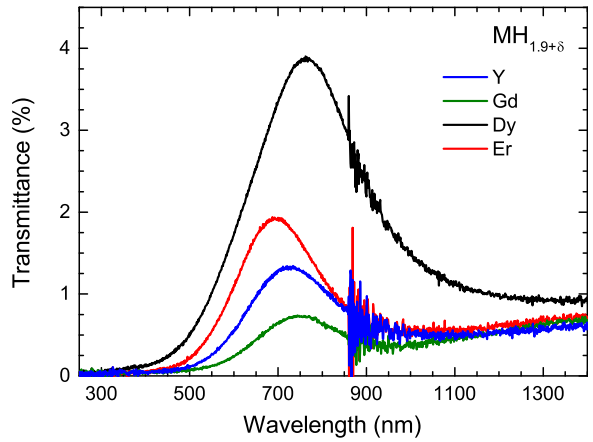

FIG. 1. Characteristic transmittance window of Y and rare-earth dihydride thin films directly prepared by reactive magnetron sputtering below the critical deposition pressure. The difference in maximum transmittance is a result of film thickness variation between 188 nm (M = Dy) and 320 nm (M = Gd).

Such a transmittance window has been reported previously for Y-La dihydride films by van Gogh *et al.*—in particular in the hydrogen poor part of the dihydride solid solution (i.e., fcc-$YH_{1.9+\delta}$).[5] It arises from a combination of weak free electron and inter-band absorption near the plasma frequency. The position (wavelength) of the dihydride window has been reported to shift with hydrogen/metal ratio[15,16] as well as Y/La ratio in alloyed hydrides.[5] We do not find any systematic correlation of the transmittance window peak wavelength with the cation size or lattice constant. Probably, this variation is an effect of minor changes in the H/M ratio, or rather free electron density, in different samples. Nevertheless, the observation of the characteristic transmittance window is a strong indicator for the presence of the metallic fcc-dihydride phase (MH_2). In conjunction with the XRD analysis (see below), this demonstrates that stable rare-earth dihydride thin films can be produced directly by reactive sputter deposition i.e., without the need for Pd capping and a separate hydrogenation step.

When the Y and lanthanide films are deposited above the critical pressure, initially they also appear black opaque inside the vacuum chamber and in an attached glove box ($p_{O2} < 1$ ppm). However, upon exposure to air, they rapidly react and become transparent. Our preliminary ion-beam analysis results indicate an oxygen content of 20–30 at. % (not shown), which is comparable to earlier reports on YO_xH_y.[6] Therefore, these transparent and photochromic materials are referred to as metal oxy-hydrides (MO_xH_y). The uptake of oxygen from air is driven by the large difference in formation enthalpy between oxides and hydrides e.g., –1895 kJ/mol[17] for bixbyite-Y_2O_3 vs. –228 kJ/mol[18,19] for YH_2. Probably, the observed deposition pressure dependent oxidation behavior is related to a higher porosity of the as-prepared MH_2 films when grown at higher pressures. The micro-structure of sputtered thin films strongly depends on the ad-atom mobility of deposited species, which is controlled by the flux of energetic particles arriving at the film surface (mainly sputtered atoms and back-reflected Ar neutrals) as well as the substrate temperature. These effects result in the well-known structure-zone-models[20] characteristic of sputtered thin films describing the formation of denser micro-structures at low deposition pressures. This is because of collisions of the energetic particles with the process gas on their way from sputter target to substrate, effectively reducing their average energy as the deposition pressure is increased. These concepts explain qualitatively our observation that a critical deposition pressure, p^*, exists such that films deposited at $p < p^*$ remain metallic dihydrides whereas films deposited above p^* transform into semiconducting oxy-hydrides upon air exposure. Experimentally, we find $p^*(YO_xH_y) \simeq 0.4$ Pa whereas $p^* \simeq 0.6$ Pa for Gd, Dy, and Er oxy-hydrides. This material dependence of p^*, and hence MH_2 film density, is likely attributed to a significant contribution of back-reflected Ar neutrals to the overall energy flux towards the growing films. Both the reflection probability and average energy of reflected Ar neutrals increase with atomic mass of the target.[21,22] Taking into account the large mass difference between the lanthanides and Y, it is therefore plausible that a higher gas pressure is required in the case of Gd, Dy, and Er to achieve similar (porous) thin film micro-structure as in YH_x allowing for air-oxidation and formation of MO_xH_y.

To investigate the effect of different cations and post-deposition oxidation on the thin film crystal structure, the lattice constants are summarized in Fig. 2. The well-known lanthanide contraction with increasing number of 4f-electrons is reflected in the systematic decrease of lattice constants of the fcc-MH_2 dihydrides (open circles) as well as the cubic bixbyite M_2O_3 oxides[17] (open triangles) with increasing atomic number. Although Y is not a lanthanide, the lattice constant of Y_2O_3 can be sorted in between Dy and Er. All films sputter deposited at pressures below p^* (Y at 0.3 Pa and Gd, Dy, and Er at 0.5 Pa) are black metallic upon deposition and remain so when exposed to air. Their diffraction patterns are consistent with the face centered cubic (fcc) structure of the CaF_2 prototype (space group Fm-3 m) characteristic of the metallic β-MH_2 phases. We find a 0.8–1.2% lattice expansion of these *directly sputtered* dihydride films (full red circles)

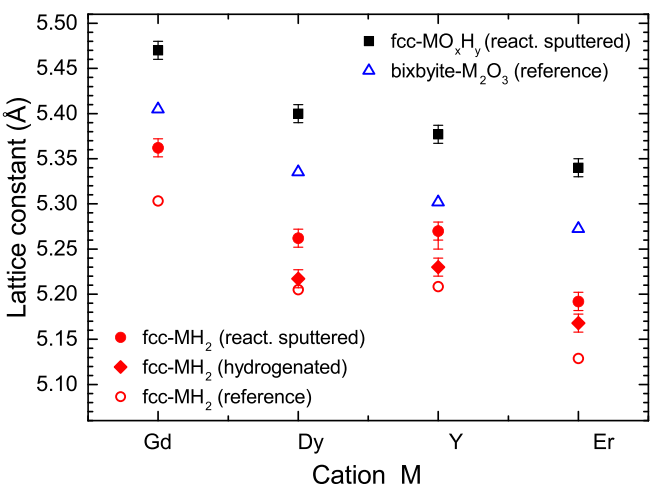

FIG. 2. Lattice constants of Yttrium and lanthanide based dihydride MH_2(red symbols), oxide M_2O_3 (blue symbols), and photochromic MO_xH_y oxy-hydride (black symbols) thin films. Experimental XRD results of the present work (full symbols) are compared to reference data taken from the ICDD-PDF database (open symbols). Note that due to the structural similarity to the fcc unit cell only 1/2 of the bixbyite M_2O_3 lattice constant is shown here.

relative to the reference values taken from ICDD-PDF (open circles). The lattice constant value of 5.27 ± 0.01 Å of sputtered yttrium hydride is in agreement with an earlier report by Mongstad *et al.*[7] In comparison, we observe significantly smaller lattice constants in Pd capped YH_2, DyH_2, and ErH_2 thin films prepared by sputtering of metal layers in pure Ar followed by a separate hydrogenation step at $p_{H2} = 1$ bar at RT (full red diamonds). These results are closer to the reference values which represent highly ordered structures obtained by hydrogenation of (bulk) metals at elevated temperatures. Since the Pd capped films were grown using the same sputter targets, substrates, pressure, and discharge power, we can rule out target impurities and energetic particle bombardment effects as the origin of the lattice expansion of the *directly sputtered* MH_2 films. Instead, it seems plausible that this effect is related to the interaction of H with the lattice. In contrast to hydrogenation, reactive sputtering can be regarded as a non-equilibrium process. Therefore, a certain amount of disorder of the H sublattice may be present in *directly sputtered* MH_2 films, i.e., a fraction H occupies the octahedral lattice sites, instead of tetrahedral sites as in the ideal fcc-MH_2 structure.

The transparent photochromic oxy-hydride MO_xH_y films grown at pressures above p^* (Y at 0.5 Pa and Gd, Dy, and Er at 0.7 Pa) retain the fcc structure but with a substantial lattice expansion of 1.9–2.8% relative to the corresponding MH_2 films sputtered below p^*. This lattice expansion is clearly attributed to the incorporation of oxygen after air exposure. We find a value of 5.38 ± 0.01 Å for YO_xH_y which is within the range of values reported in earlier publications.[7,8] Remarkably, the MO_xH_y lattice constants follow the trend of the lanthanide contraction of the bixbyite-M_2O_3 compounds (open triangles).[17] Hence, cation substitution allows for tuning of the unit cell dimensions of rare-earth based MO_xH_y and could thereby enable tailoring of optical and electrical properties. In addition, for each cation M the absolute lattice constant of the MO_xH_y is even larger than that of the corresponding structural unit of the bixbyite-M_2O_3 unit cell. While this effect is puzzling at first, it can be explained by a large concentration of H^- ions present in the fcc-MO_xH_y structure. Considering charge neutrality and attributing formal valencies of M^{3+} and O^{2-}, the valence of H in MO_xH_y can be estimated from the chemical composition data obtained by ion beam analysis (not shown). In fact, we find that charge neutrality is obeyed (within measurement accuracy) only if we assign a valence of –1 to H, whereas assuming H in the form of H^+ or OH^- would result in violation of the charge neutrality. Interestingly, Miniotas *et al.* arrived at the same conclusion about the role of H in GdO_xH_y thin films.[23] Hence, in a simplified picture, we can regard the expanded fcc-MO_xH_y structure as a bixbyite-M_2O_3 structure where O^{2-} is substituted by H^- with some additional H^- occupying the structural O vacancies of the bixbyite lattice. Further dedicated experiments are required to directly confirm the presence of H^- ions in MO_xH_y materials.

All the oxy-hydrides we have investigated show photochromic behavior. The changes of spectral transmittance of a set of Y and lanthanide MO_xH_y thin films due to UV irradiation are compared in Fig. 3(a). Employing the Tauc plot method, we find that YO_xH_y has a bandgap of $E_g = (2.60 \pm 0.05)$ eV consistent with earlier reports.[6,7] The lanthanide oxy-hydrides

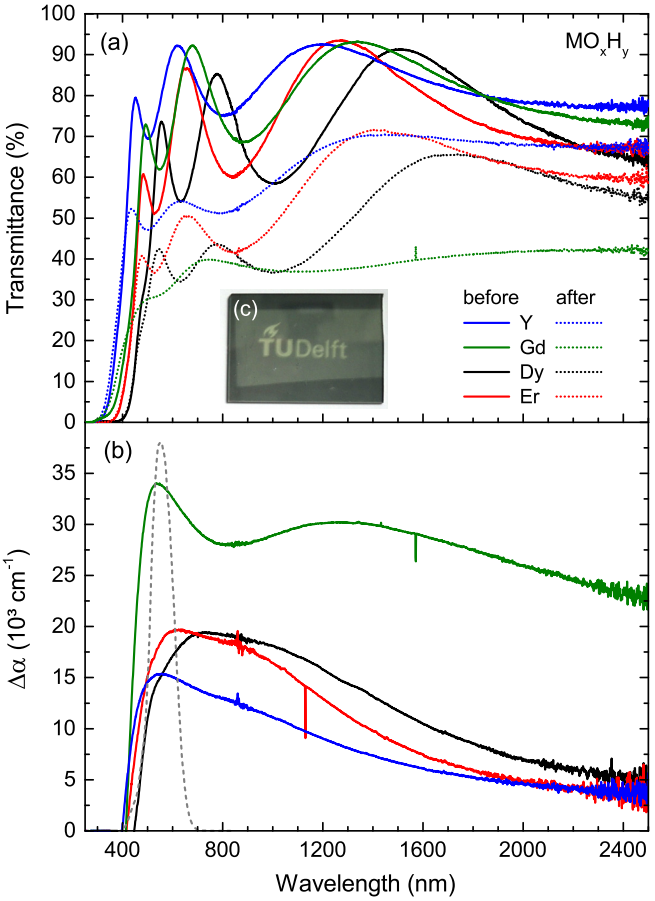

FIG. 3. Photochromic response of Y and lanthanide oxy-hydride thin films (thickness between 270 and 350 nm) after 5 h of UV illumination at 5070 μWcm^{-2}. (a) Transmittance before (solid lines) and after photo-darkening (dotted lines). (b) Corresponding change of absorption coefficient. Note that the absorption coefficients are calculated taking into account the reflectance $R(\lambda)$ (not shown) using the expression $T(\lambda) = [1-R(\lambda)]\exp[-\alpha(\lambda)d]$.[24] The normalized human eye luminosity function according to Sharpe *et al.*[25] is shown as a dashed curve in (b). (c) Photograph of a 500 nm YO_xH_y film on glass after UV illumination through shadow masks illustrating the transparent "bleached" state (letters) and two levels of photochromic contrast.

have lower bandgaps of 2.40 eV (ErO_xH_y) and 2.25 eV (GdO_xH_y and DyO_xH_y). This confirms the general notion that the bandgap of the MO_xH_y oxy-hydrides is substantially lower than that of the corresponding bixbyite-M_2O_3 oxides (4.9–5.4 eV).[17,26] Furthermore, the best Tauc fits were obtained with an exponent of 1/2 indicating that the bandgaps of all oxy-hydrides are *indirect* (see Fig. S3, supplementary material). Using an exponent of 2 in the Tauc plot (assuming a direct bandgap) would result in erroneous band-gap values approximately 1 eV larger than given above. Perhaps the only comparison available is a report by Miniotas *et al.* stating $E_g = (3.2 \pm 0.2)$ eV for a $GdO_{0.6}H_{1.53}$ (19 at. % O) thin film.[23] Since the oxygen content is very close to our GdO_xH_y material and not all analysis details were disclosed, they very likely overestimated the bandgap value by assuming a direct transition. We did not observe any change of E_g due to photodarkening. For all MO_xH_y films, UV illumination causes a decrease of transmittance in a wide spectral range from E_g to 2500 nm and beyond. The corresponding difference in the optical absorption coefficient is shown in Fig. 3(b) and allows for a direct comparison of the photochromic effect. A broad maximum of the photochromic response is observed in each

material. In the case of YO_xH_y, this maximum is centered at 550 nm explaining the color-neutral appearance of photo-darkening, whereas for M = (Dy, Er), the maxima are red-shifted towards the long-wavelength limit of the human eye luminosity function. While in the case of M = (Y, Dy, and Er) the photochromic effect is similar in magnitude ($\Delta\alpha_{max} \simeq 20\,000\,cm^{-1}$) and decreases towards the NIR, GdO_xH_y shows an unusually strong photochromic response extending far into the NIR. This unique effect could be related to a large increase in free-electron absorption during photo-darkening. In fact, the resistivity of YO_xH_y has been reported to decrease (increase) reversibly along with photo-darkening (bleaching).[6] Further experiments are planned to confirm this hypothesis.

We define the (absolute) photochromic contrast $\Delta T(\lambda,t)$ as the change of transmittance with respect to the initial value, T_0, in the bleached state before UV-illumination, i.e., $\Delta T(\lambda, t) = T_0(\lambda, 0) - T(\lambda, t)$. In general, for each material the optical contrast is a function of film thickness and illumination conditions. Thus, in order to compare the photochromic performance of the different oxy-hydride materials, another set of samples of the same thickness (300 nm) have been illuminated under the same conditions followed by bleaching in dark conditions at room temperature. A comparison of the time dependent and spectral averaged contrast, $\langle\Delta T\rangle$, is shown in Fig. 4. As expected from Fig. 3(a), YO_xH_y is the most transparent material in the bleached state ($\langle\Delta T_0\rangle = 79.8\%$) while the lanthanide oxy-hydrides are initially less transparent ($\langle\Delta T_0\rangle = 67.9$–$71.3\%$). These differences are mainly due to the lower bandgap and higher sub-bandgap absorption (Urbach's tail)[27] present in the lanthanide oxy-hydrides (see Fig. S3, supplementary material). During photo-darkening, all materials initially show a fast (nearly exponential) increase of contrast followed by a slow change with nearly linear behavior until the light source is switched off after about 8 hours. In particular, GdO_xH_y and YO_xH_y show a fast photochromic response and reach large optical contrast values of $\langle\Delta T\rangle = (25$–$33)\%$ already after 15 min of illumination. While the maximum optical contrast values of Y, Dy, and Er are comparable $\langle\Delta T\rangle = (33$–$37)\%$, a significantly higher maximum contrast of $\langle\Delta T\rangle = 45.5\%$ is observed for Gd. According to Fig. 3(b), this enhanced photochromic contrast is a result of the large absorption coefficient change of GdO_xH_y especially in the NIR range. The kinetics of $\langle\Delta T(t)\rangle$ during bleaching are well described by an exponential decay function $\langle\Delta T(t)\rangle \propto \exp(-t/\tau_B)$ using the (thermal) bleaching time constant, τ_B, as a fitting parameter. We find that DyO_xH_y bleaches the fastest ($\tau_B = 215 \pm 15$ min), followed by Y and Gd, while ErO_xH_y shows the slowest bleaching rate of all materials ($\tau_B = 1260 \pm 80$ min). Our ongoing studies indicate that the bleaching kinetics not only depend on the cation but also on sputter deposition parameters and illumination conditions. Therefore, additional experimentation is required for a more quantitative comparison.

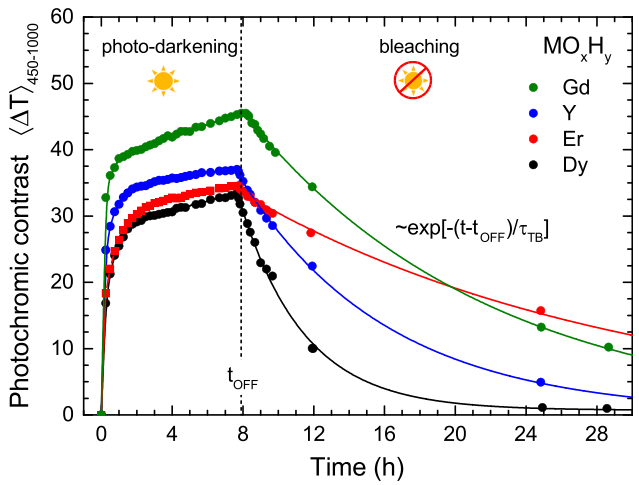

FIG. 4. Wavelength averaged optical contrast of Y and lanthanide oxy-hydride films ($d = 300$ nm) during UV illumination at 5860 μW cm^{-2} followed by (thermal) bleaching in the dark. The spectral averaging between 450 and 1000 nm effectively reduces the influence of optical interference patterns on $\Delta T(t)$.

In conclusion, our work demonstrates that (i) stable lanthanide dihydride thin films can be grown directly by reactive magnetron sputtering, (ii) lanthanide oxy-hydride thin films exhibit a photochromic effect similar to YO_xH_y suggesting a common physical mechanism, (iii) initial transmittance, photochromic contrast values and photo-darkening speed are promising for applications such as smart windows, (iv) cation alloying is a viable approach to tailor the photochromic properties of MO_xH_y because they share the same fcc-structure while optical bandgap, photochromic contrast, and bleaching rate vary substantially between different cations. Based on the presented results, we predict that the oxy-hydrides of the remaining rare-earths (incl. Sc) are also potentially photochromic. Systematic synthesis and exploration of their properties might lead to further insight into the physical mechanisms governing the photochromic effect in this class of materials.

See supplementary material for further details regarding XRD analysis, XRD patterns of MH_2 and MO_xH_y thin films, optical spectroscopy methods, and bandgap determination.

This work was financially supported by the Dutch Technology Foundation STW, which is part of the Netherlands Organization for Scientific Research (NWO), and which is partly funded by the Ministry of Economic Affairs. We are grateful to E. ten Have for contributions to the optical measurements.

[1]J. N. Huiberts, R. Griessen, J. H. Rector, R. J. Wijngaarden, J. P. Dekker, D. G. Degroot, and N. J. Koeman, Nature **380**, 231 (1996).
[2]J. N. Huiberts, J. H. Rector, R. J. Wijngaarden, S. Jetten, D. de Groot, B. Dam, N. J. Koeman, R. Griessen, B. Hjörvarrson, S. Olafsson, and Y. S. Cho, J. Alloys Compd. **239**, 158 (1996).
[3]Y. Pivak, H. Schreuders, and B. Dam, J. Mater. Chem. **22**, 24453 (2012).
[4]E. S. Kooij, A. T. M. van Gogh, D. G. Nagengast, N. J. Koeman, and R. Griessen, Phys. Rev. B **62**, 10088 (2000).
[5]A. T. M. van Gogh, D. G. Nagengast, E. S. Kooij, N. J. Koeman, J. H. Rector, R. Griessen, C. F. J. Flipse, and R. J. J. G. A. M. Smeets, Phys. Rev. B **63**, 195105 (2001).
[6]T. Mongstad, C. Platzer-Bjorkman, J. P. Maehlen, L. P. Mooij, Y. Pivak, B. Dam, E. S. Marstein, B. Hauback, and S. Z. Karazhanov, Sol. Energy Mater. Sol. Cells **95**, 3596 (2011).
[7]T. Mongstad, C. Platzer-Bjorkman, S. Z. Karazhanov, A. Holt, J. P. Maehlen, and B. C. Hauback, J. Alloys Compd. **509**, S812 (2011).
[8]J. Montero, F. A. Martinsen, M. Lelis, S. Z. Karazhanov, B. C. Hauback, and E. S. Marstein, "Photochromic mechanism in oxygen-containing yttrium hydride thin films: an optical perspective," Sol. Energy. Mater. Sol. Cells (in press).
[9]H. Tian and S. Yang, Chem. Soc. Rev. **33**, 85 (2004).

[10]K. Sasaki and T. Nagamura, Appl. Phys. Lett. **71**, 434 (1997).
[11]R. Pardo, M. Zayat, and D. Levy, Chem. Soc. Rev. **40**, 672 (2011).
[12]G. P. Smith, J. Mater. Sci. **2**, 139 (1967).
[13]R. J. Araujo, Contemp. Phys. **21**, 77 (1980).
[14]T. Mongstadt, Ph.D. thesis, University of Oslo, Norway, 2012.
[15]M. Sakai, T. Kontani, O. Nakamura, K. Takeyama, Y. Uwatoko, Y. Obi, and K. Takanashi, Jpn. J. Appl. Phys., Part 1 **43**, 681 (2004).
[16]A. T. M. van Gogh, Ph.D. thesis, Vrije Universiteit Amsterdam, The Netherlands, 2001.
[17]G. Adachi and N. Imanaka, Chem. Rev. **98**, 1479 (1998).
[18]L. N. Yannopoulos, R. K. Edwards, and P. G. Wahlbeck, J. Phys. Chem. **69**, 2510 (1965).
[19]Y. Fukai, *The Metal-Hydrogen System: Basic Bulk Properties*, 2nd ed. (Springer, Berlin, Heidelberg, Germany, 2005), Vol. 2.
[20]A. Anders, Thin Solid Films **518**, 4087 (2010).
[21]T. Drüsedau, T. Bock, T. John, F. Klabunde, and W. Eckstein, J. Vac. Sci. Technol. **17**, 2896 (1999).
[22]W. Eckstein and J. P. Biersack, Z. Phys. B: Condens. Matter **63**, 471 (1986).
[23]A. Miniotas, B. Hjörvarsson, L. Douysset, and P. Nostell, Appl. Phys. Lett. **76**, 2056 (2000).
[24]M. Cesaria, A. P. Caricato, and M. Martino, J. Opt. **14**, 105701 (2012).
[25]L. T. Sharpe, A. Stockman, W. Jagla, and H. Jägle, J. Vision **5**(3), 948–968 (2005).
[26]A. V. Prokofiev, A. I. Shelykh, and B. T. Melekh, J. Alloys Compd. **242**, 41 (1996).
[27]E. A. Davis and N. F. Mott, Philos. Mag. **22**, 0903 (1970).